VELOCITY DETERMINATIONS IN PULSATING PIPE FLOWS

By

Byron Paul Whitehurst

United States
Naval Postgraduate School

THESIS

VELOCITY DETERMINATIONS
IN PULSATING PIPE FLOWS

by

Byron Paul Whitehurst

December 1970

Velocity Determinations in Pulsating Pipe Flows

by

Byron Paul Whitehurst
Lieutenant Commander, United States Navy
B.S., Miami University, 1962

Submitted in partial fulfillment of the
requirements for the degree of

MASTER OF SCIENCE IN MECHANICAL ENGINEERING

from the

NAVAL POSTGRADUATE SCHOOL
December 1970

ABSTRACT

A study of the fluctuating velocity field in the developing region of a pulsating pipe flow is presented.

Theoretically, three separate determinations of radial and axial perturbation velocity profiles were calculated involving varying degrees of analytical simplification.

Experimentally, pulsating disturbances were created by a sinusoidal pressure wave exciter installed at the outlet of a 1.5 inch circular wind tunnel facility. Cross-wire anemometer measurements of the pulsating velocity components compared favorably with the parallel theoretical results. Likewise, experimental determinations of the phase angles between velocity and pressure signals compared favorably with analytical values.

TABLE OF CONTENTS

LIST OF TABLES

LIST OF FIGURES

NOMENCLATURE

b_0, b_1, b_2, b_3	Constants, coefficients of the polynomial approximation of the velocity profile
d	Inside diameter of the pipe
P	Pressure
r	Radial coordinate
r_0	Radius of the pipe
R	Reynolds number
t	Time
$\bar{U}$	Mean velocity in the pipe
U_M	Maximum velocity in the pipe
u	Axial component of velocity
v	Radial component of velocity
x	Axial coordinate
ν	Kinematic viscosity
ρ	Density
ϕ	Angle of phase shift

ACKNOWLEDGEMENT

The author wishes to express his profound gratitude to Professor T. Houlihan for his guidance, encouragement, and infectious enthusiasm during the course of this investigation. A special note of appreciation is also given to Messrs. K. Mothersell, J. McKay, J. Beck, and G. Baxter of the Mechanical Engineering Machine Shop for their generous assistance in the construction of the experimental apparatus.

The author is especially grateful to his wife, who was patient and understanding throughout the period of this study.

I. INTRODUCTION

The development of flow in the inlet region of a circular cylindrical tube has been a subject of interest since the time of Hagen (1839) and Poiseuille (1841). Osborne Reynolds (1883) conducted extensive investigations into the stability of pipe flow, and this area has become a classic problem with a sizable amount of literature published. However, the study of fluid flow through a rigid tube under the influence of a periodic pressure difference is more limited.

The theoretical study of pulsating, laminar pipe flow was primarily given by Th. Sexl [1] and S. Uchida [2]. Experimental data are limited to the works of Atabek, Chang, and Fingerson [3] and the results of Florio and Meuller [4]. With the introduction of the modern computer, several attempts have been made to solve the problem by numerical methods. The most recent work in this regard is that of Lew and Fung [5]. In the theoretical analysis the main problem has been the non-linear convective acceleration term in the Navier-Stokes equation. Uchida [2] was able to apply linear theory for the fully developed laminar pulsating flow. Lew and Fung [5] found this linearization to be valid in the entry region for high Reynolds numbers. However, this assumption leads to significant errors for small Reynolds numbers (the area of most interest).

The present investigation was undertaken to study the fluctuating velocity field which arises in the developing region of a rigid walled conduit due to an imposed sinusoidal pressure gradient. Additionally, results were sought concerning any phase differences between the velocity and pressure signals with a view toward later stability determinations.

II. THEORETICAL ANALYSIS

A. SOLUTION # 1 OF PULSATING FLOW EQUATIONS

For oscillatory flow in a circular pipe, the Navier-Stokes equations must be solved for $\tilde{u}$ and $\tilde{v}$, the fluctuating velocity components, as functions of three variables (r,x,t). The velocities, $\tilde{u}$ and $\tilde{v}$, are independent of ϕ, the azimuthal coordinate. The applicable equations from Schlichting [6] are:

$$\frac{\partial u}{\partial t} + u\frac{\partial u}{\partial x} + v\frac{\partial u}{\partial r} = -\frac{1}{\rho}\frac{\partial P}{\partial x} + \nu\left\{\frac{\partial^2 u}{\partial r^2} + \frac{1}{r}\frac{\partial u}{\partial r} + \frac{\partial^2 u}{\partial x^2}\right\} \qquad (1)$$

$$\frac{\partial v}{\partial t} + u\frac{\partial v}{\partial x} + v\frac{\partial v}{\partial r} = -\frac{1}{\rho}\frac{\partial P}{\partial x} + \nu\left\{\frac{\partial^2 v}{\partial r^2} + \frac{1}{r}\frac{\partial v}{\partial r} + \frac{\partial^2 v}{\partial x^2} - \frac{v}{r^2}\right\} \qquad (2)$$

The continuity equation is:

$$\frac{\partial u}{\partial x} + \frac{\partial v}{\partial r} + \frac{v}{r} = 0 \qquad (3)$$

It is assumed that $u = \bar{u} + \tilde{u}$, $p = \bar{p} + \tilde{p}$, and $v = \tilde{v}$ where $\bar{u}$ and $\bar{p}$ are the steady components and $\tilde{u}$, $\tilde{v}$, and $\tilde{p}$ are the pulsating components.

After linearization, two additional assumptions are made, namely, (1) that $\tilde{p}$ is applied across the full cross-section of the tube, i.e., $\tilde{p}$ is independent of r, and (2) that the gradient of $\tilde{v}$ in the x direction is mild compared with the gradient in the r direction.

The resulting equations are:

$$\frac{\partial \tilde{v}}{\partial t} + \bar{u}\,\frac{\partial \tilde{v}}{\partial x} = \nu \left\{ \frac{\partial^2 \tilde{v}}{\partial r^2} + \frac{1}{r}\,\frac{\partial \tilde{v}}{\partial r} - \frac{\tilde{v}}{r^2} \right\} \tag{4}$$

$$\frac{\partial \tilde{u}}{\partial t} + \bar{u}\,\frac{\partial \tilde{u}}{\partial x} + \tilde{v}\,\frac{\partial \bar{u}}{\partial r} = -\frac{1}{\rho}\,\frac{\partial \tilde{P}}{\partial x} + \nu\,\nabla^2\,\tilde{u} \tag{5}$$

$$\frac{\partial \tilde{u}}{\partial x} + \frac{\partial \tilde{v}}{\partial r} + \frac{\tilde{v}}{r} = 0 \tag{6}$$

Substitution of (6) into (5) yields

$$\nu\,\nabla^2\,\tilde{u} - \frac{1}{\rho}\,\frac{\partial \tilde{P}}{\partial x} - \frac{\partial \tilde{u}}{\partial t} = -\bar{u}\,\frac{\partial \tilde{v}}{\partial r} - \frac{\bar{u}\tilde{v}}{r} + \tilde{v}\,\frac{\partial \bar{u}}{\partial r} \tag{7}$$

The left side of equation (7) is recognized as that treated by Uchida [2] and the right side of (7) is known if $\tilde{v}$ and $\bar{u}$ are known.

By assuming $\tilde{v} = R(r)X(x)e^{i(Nt+\phi)}$, equation (4) may be solved by separation of variables. This technique yields

$$\frac{X'}{X} = \frac{\nu}{\bar{u}} \left\{ \frac{R''}{R} + \frac{R'}{rR} - \frac{1}{r^2} - \frac{iN}{\nu} \right\} = -\omega^2 \tag{8}$$

for which the X solution is

$$X = C_1 e^{-\omega^2 x} \tag{9}$$

and the R solution after assuming a series representation becomes

$$R = a_o r \left[1 - \frac{\beta r^2}{8} - \left(\frac{8\alpha - \beta^2}{192} \right) r^4 + \frac{\beta}{192} \left(\frac{2\alpha}{3} - \beta^2 \right) r^6 + \frac{1}{192} \left(\frac{\alpha^2}{10} - \frac{\alpha\beta 2}{48} + \frac{\beta^3}{80} \right) r^8 + \ldots \right] \tag{10}$$

Therefore the complete solution for $\tilde{v}$ is

$$\tilde{v} = C_1 a_o r\, e^{-\omega^2 x}\, e^{i(Nt+\phi)} \left[1 - \frac{\beta r^2}{8} - \left(\frac{8\alpha-\beta^2}{192}\right) r^4 + \frac{\beta}{192}\left(\frac{2\alpha}{3} - \beta^2\right) r^6 + \frac{1}{192}\left(\frac{\alpha^2}{10} - \frac{\alpha\beta^2}{48} + \frac{\beta^3}{80}\right) r^8 + \ldots\right] \tag{11}$$

where

$$\alpha = \frac{-\omega^2 U_o}{\nu r^2} \tag{12}$$

$$\beta = \frac{\omega^2 U_o - iN}{\nu} \tag{13}$$

and $-\omega^2$ is the constant introduced in the separation of variable technique. Now that a solution for $\tilde{v}$ is known, equation (7) may be solved. By substituting equation (11) into (7) and further assuming

$$\bar{u} = b_o + b_1 r + b_2 r^2 \tag{14}$$

$$-\frac{1}{\rho}\frac{\partial \tilde{p}}{\partial x} = -\nu\, Pn\, e^{int},\ \tilde{u} = \tilde{u}(r)\, e^{int} \tag{15}$$

equation (7) becomes a zero order non-homogeneous Bessel equation of the form

$$\tilde{U}'' + \frac{1}{r}\tilde{U}' - \frac{iN}{\nu}\tilde{U} = P_N + \frac{e^{-int}}{\nu}\left\{\tilde{v}\frac{\partial \bar{u}}{\partial r} - \bar{u}\frac{\tilde{v}}{r} - \frac{\bar{u}\tilde{v}}{r}\right\} \tag{16}$$

The relationship in equation (14) allows determinations in the developing region to be made. The relationships in equation (15) concerns an oscillating axial pressure gradient and a resultant oscillatory axial velocity fluctuation.

The complimentary solution of equation (16) is

$$\tilde{U}_c = C_2 J_0(z) + C_3 Y_0(z) \tag{17}$$

where $z = \sqrt{-i}\,\lambda r$ and $\lambda = \sqrt{\frac{N}{\nu}}$.

The particular solution is obtained by the method of variation of parameters (Wylie[7]).

$$\tilde{U}_p = u_1 y_1 + u_2 y_2 \tag{18}$$

where $y_1 = J_0(z)$ and $y_2 = Y_0(z)$, and

$$u_1' = \frac{-y_2}{y_1 y_2' - y_2 y_1'} R(r,x,t) \tag{19}$$

$$u_2' = \frac{y_1}{y_1 y_2' - y_2 y_1'} R(r,x,t) \tag{20}$$

with

$$R(r,x,t) = P_N + \frac{e^{-int}}{\nu}\left\{\tilde{v}\,\frac{\partial \bar{u}}{\partial r} - \bar{u}\,\frac{\partial \tilde{v}}{\partial r} - \frac{\bar{u}\tilde{v}}{r}\right\} \tag{21}$$

The denominator of u_1' and u_2' is the Wronskian of (y_1, y_2) (Abramowitz and Stegun [8])

$$W(y_1, y_2) = \frac{2}{\pi z} \tag{22}$$

Therefore

$$u_1' = \frac{-\pi z}{2} Y_0(z)\; R(r,x,t) \tag{23}$$

$$u_2' = \frac{\pi z}{2} J_0(z)\; R(r,x,t) \tag{24}$$

Entering the formulations for $\bar{u}$ and $\tilde{v}$ into the expression for $R(r,x,t)$ and then substituting the resultant expression equations (23) and (24) yields

$$u_1 = e^{i\phi}\left[-\frac{\pi P_N}{2}\int z\ Y_0(z)\right. \tag{25}$$

$$+ \lambda_1 \int z\ Y_0(z) + \lambda_2 \int z^2\ Y_0(z)$$

$$- \lambda_3 \int z^3\ Y_0(z) - \lambda_4 \int z^4\ Y_0(z)$$

$$- \lambda_5 \int z^5\ Y_0(z) - \lambda_6 \int z^6\ Y_0(z)$$

$$- \lambda_7 \int z^7\ Y_0(z) - \lambda_7 \int z^7\ Y_0(z)$$

$$\left. - \lambda_9 \int z^9\ Y_0(z) + \ldots\right]$$

where the various constants are listed in Table I.

Similarly

$$u_2 = e^{i\phi}\left[\frac{\pi P_N}{2}\int z\ J_0(z) -\right. \tag{26}$$

$$\lambda_1 \int z\ J_0(z) - \lambda_2 \int z\ J_0(z)$$

$$+ \lambda_3 \int z^3\ J_0(z) + \lambda_4 \int z^4\ J_0(z)$$

$$+ \lambda_5 \int z^5\ J_0(z) + \lambda_6 \int z^6\ J_0(z)$$

$$+ \lambda_7 \int z^7\ J_0(z) + \lambda_8 \int z^8\ J_0(z)$$

$$\left. + \lambda_9 \int z^9\ J_0(z) + \ldots\right]$$

After integration to obtain the expressions for u_1 and u_2 and substitution back into equation (18), the complete expression for $\tilde{u}$ is obtained.

$$\tilde{u} = C_2 J_0(z) + P_N e^{i\phi} - \lambda_i e^{i\phi} \left(\frac{2}{\pi}\right) \tag{27}$$

$$- \lambda_2 e^{i\phi} \left[\frac{2z}{\pi} - J_0(z) \int Y_0(z) + Y_0(z) \int J_0(z)\right] + \lambda_3 e^{i\phi} \left[\frac{2}{\pi} (z^2-4)\right] + \lambda_4 e^{i\phi} \left[\frac{2}{\pi} (z^3-9z) + 9\left(\int J_0(z) - \int Y_0(z)\right)\right]$$

$$+ \lambda_5 e^{i\phi} \left[\frac{2}{\pi} (z^4-6z^2-16)\right] + \lambda_6 e^{i\phi} \left[\frac{2}{\pi} (z^5-25z^3+225z) + 225\left(\int Y_0(z) - \int J_0(z)\right)\right]$$

$$+ \lambda_7 e^{i\phi} \left[\frac{2}{\pi} (z^6-36z^4+208z^2-96)\right] + \lambda_8 e^{i\phi} \left[\frac{2}{\pi} (z^7-49z^5+1225z^3) - 11{,}025z) + 11{,}025\left(\int J_0(z) - \int Y_0(z)\right)\right]$$

$$+ \lambda_9 e^{i\phi} \left[\frac{2}{\pi} (z^8-64z^6+2304z^4-38{,}864z^2+147{,}456)\right]$$

The constant C_3 is made equal to zero by the boundary condition that $\tilde{u}$ must be everywhere finite. The constant C_2 is solved for by the boundary condition that $\tilde{u} = 0$ at $r = r_0$.

The difficulty involved with this expression is obvious. Thus a second attempt at a theoretical solution was made to obtain a more manageable solution for the ease of calculation.

B. SOLUTION # 2 OF PULSATING FLOW EQUATIONS

In this second phase of the theoretical analysis, the assumption that $\tilde{v}$ is independent of x is made. Thus, equation (4) becomes

$$\frac{\partial \tilde{v}}{\partial t} = \nu \left\{ \frac{\partial^2 \tilde{v}}{\partial r^2} + \frac{1}{r} \frac{\partial \tilde{v}}{\partial r} - \frac{\tilde{v}}{r^2} \right\} \tag{28}$$

Again, an oscillatory form for $\tilde{v}$ (now independent of x) is assumed, namely $\tilde{v} = R(r)\, e^{i(Nt+\phi)}$. Substitution of this formulation into equation (28) yields a first order Bessel equation

$$R'' + \frac{1}{r} R' - \left(\frac{1}{r^2} + \frac{iN}{\nu} \right) R = 0 \tag{29}$$

with the solution

$$R(r) = J_1 \left(i^{3/2} \lambda r \right) \tag{30}$$

Incorporating this new expression for $\tilde{v}$ alters the results for u_1 and u_2 of the particular solution of $\tilde{u}$. The new expression for u_2 becomes

$$u_2 = \frac{\pi P_N e^{i\phi}}{2} z J_1(z) - \frac{2\lambda_{23} e^{i\phi}}{3} z^3 J_0(z) J_1(z) \qquad (31)$$

$$+ e^{i\phi}\left[\frac{\lambda_{24}}{2} - \frac{\lambda_{23} z^4}{3} - \frac{z^2}{2} - \lambda_{22} - \frac{\lambda_{22} z^2}{2}\right] J_0^2(z)$$

$$+ e^{i\phi}\left[\frac{\lambda_{21} z^2}{2} - \lambda_{22} z^2 - \frac{\lambda_{23} z^4}{3} - \lambda_{23} z^2 - \frac{\lambda_{25} z^2}{2}\right] J_1^2(z)$$

As $J_\nu(x)$ and $Y_\nu(x)$ are both cylinder functions, the expression for u_1 can similarly be expressed by substituting Y_i for J_i. The constants λ_{2j} are tabulated in Table II. The final expression for $\tilde{u}$ thus becomes

$$\tilde{u} = C_2 J_0(z) + u_1 J_0(z) + u_2 Y_0(z) \qquad (32)$$

The immensity of $\tilde{u}$ has been somewhat reduced. However, it was felt that additional assumptions would yield a very workable solution.

C. SOLUTION # 3 OF PULSATING FLOW EQUATIONS

After obtaining the two previous solutions for $\tilde{u}$, a more simplified expression was still desired. An order of magnitude analysis for $\tilde{u}$ near the wall and for $\tilde{u}$ near the centerline was made, these being the two main areas of interest during the investigation. These order of magnitude determinations did lead to the finding of a simplified solution applicable across the entire cross section of the pipe.

The expression for $\tilde{v}$ is

$$\tilde{v} = C_1 e^{i(Nt+\phi)} J_1(z) \qquad (33)$$

Based on the boundary condition that $\tilde{v} = 0$ at $r = r_0$

$$R\, C_1\, e^{i(Nt+\phi)}\, J_1(i^{3/2}\, \lambda r_0) = 0 \tag{34}$$

which is satisfied either by $C_1 = 0$ or by

$$R\, e^{i(Nt+\phi)}\, J_1(i^{3/2}\, \lambda r_0) = 0 \tag{35}$$

Neglecting the trivial solution, then

$$R\, e^{i(Nt+\phi)}\, J_1(i^{3/2}\, \lambda r_0) = 0 \tag{36}$$

which leads to

$$\cos(Nt+\phi)\, \mathrm{ber}_1\, \lambda r_0 - \sin(Nt+\phi)\, \mathrm{bei}_1\, \lambda r_0 = 0 \tag{37}$$

or simplified

$$\tan(Nt+\phi) = \frac{\mathrm{ber}_1(x_0)}{\mathrm{bei}_1(x_0)} \tag{38}$$

where $x_0 = \lambda r_0$. This form suggests a phase angle dependence upon both time and frequency. For t=0, the dependence of phase angle upon frequency of oscillation is shown in Figure 1. The constant C_1 in this eigenvalue formulation is indeterminate because of the linearity of the problem. However, as in all such cases, it is the form rather than the amplitude of the perturbation velocity which is of interest. With ϕ thus determined from these eigenvalue considerations, $\tilde{v}$ is of the form $\tilde{v} = e^{i(Nt+\phi)}\, J_1(z)$ where the arbitrary constant has been set equal to unity for calculation purposes.

Determinations upon $\tilde{u}$ arise from equation (7)

$$\nu \nabla^2 \tilde{u} - \frac{1}{\rho} \frac{\partial \tilde{P}}{\partial x} - \frac{\partial \tilde{u}}{\partial t} = - \bar{u} \frac{\partial \tilde{v}}{\partial r} - \frac{\bar{u}\tilde{v}}{r} + \tilde{v} \frac{\partial \bar{u}}{\partial r} \tag{39}$$

Near the wall, the velocities $\bar{u}$ and $\tilde{v}$ appearing on the right side of equation (39) approach zero. The velocity gradients, $\frac{\partial \bar{u}}{\partial r}$ and $\frac{\partial \tilde{v}}{\partial r}$, though large, are finite. Thus, near the wall, equation (7) becomes that treated by Uchida, namely,

$$\nu \nabla^2 \tilde{u} - \frac{1}{\rho} \frac{\partial \tilde{P}}{\partial x} - \frac{\partial u}{\partial t} = 0 \tag{40}$$

The resultant solution of (40) with $x = \lambda r$ is

$$\tilde{u}_{WALL} = e^{int} \frac{P_N \nu}{iN} \left\{ \frac{J_0(i^{3/2}x)}{J_0(i^{3/2}x_0)} - 1 \right\} \tag{41}$$

Near the centerline, $\bar{u}$ is maximum, $\tilde{v}$ is zero and $\frac{\tilde{v}}{r}$ approaches a value of $\frac{C_1 e^{i\phi}}{2}$. Likewise, here $\frac{\partial \bar{u}}{\partial r}$ equals zero and $\frac{\partial \tilde{v}}{\partial r}$ approaches a value of $\frac{C_1 e^{i\phi}}{2}$. Thus, near the centerline, equation (7) reduces to

$$\nu \nabla^2 \tilde{u} - \frac{1}{\rho} \frac{\partial \tilde{P}}{\partial x} - \frac{\partial \tilde{u}}{\partial t} = - \bar{U}_{MAX} C_1 e^{i\phi} \tag{42}$$

The solution of this non-homogeneous Bessel equation is

$$\tilde{u}_{C/L} = \frac{P_N \nu e^{int}}{N} \left\{ \frac{J_0(i^{3/2}x)}{iJ_0(i^{3/2}x_0)} + i + \frac{C_1 i e^{i\phi} \bar{U}_{MAX}}{P_N} \right\} \tag{43}$$

In this expression for $\tilde{u}$, the last term is negligible compared to the first two. Thus, a complete solution for $\tilde{u}$ applicable to the entire pipe cross-section is

$$\tilde{u} = \frac{P_N \nu e^{int}}{iN} \left\{ \frac{J_0(i^{3/2}x)}{J_0(i^{3/2}x_0)} - 1 \right\} \tag{44}$$

This last form is equivalent to Uchida's final result for the axial fluctuation velocity component. Additionally, the companion normalized ($C_1 = 1$) radial fluctuation velocity component is

$$\tilde{v} = e^{i(nt+\phi)} J_1 (i^{3/2}x) \tag{45}$$

III. EXPERIMENTAL ANALYSIS

A. EXPERIMENTAL APPARATUS

The experimental trials were conducted in a horizontal Lucite tube 1.5 inches I.D. and 45 feet (300 diameters) long. A centrifugal fan was used to pull air from the stagnation conditions in the plenum chamber through the pipe and pulsator assembly. The inlet chamber consisted of a rectangular box three feet square in cross-section and four feet in length; the inlet chamber was fitted internally with five 6-24 mesh wire screens to eliminate inlet turbulence effects. Joining the plenum chamber and the tube was a two foot long settling chamber. The well rounded inlet horn was a quarter-section of a 9 inch by 18 inch ellipse molded of fiber glass and polished smooth. The tube, rectangular inlet chamber, and settling chamber were leveled and aligned to eliminate any curvature effect.

The pulsator assembly consisted of a sinusoidal oscillating piston arrangement driven by a MB 1250 Exciter. The pulsator was located at the end of the Lucite pipe immediately prior to the centrifugal suction fan. The piston arrangement consisted of a 12 inch diameter disc reciprocating over an 11 inch diameter opening to the atmosphere within the 13 inch cubical outlet chamber. The pulsating pressure signal was created by vibrating the piston in a direction perpendicular to the direction of the main flow velocity.

Velocity measurements were performed with a 1248-L-T 1.5-6 Thermo-Systems Inc. type cross-wire multi-sensor probe and associated electronics. The hot wire probe could be inserted at measuring ports located at 16, 20, 32, 40, 48, 56, and 272 diameters downstream of the entrance.

In all cases, the hot wire probes were mounted in a transverse micrometer mechanism, which was capable of placing the sensor to within .001 inch of any desired radial position except at the wall. Probe configuration limited placement at the wall to within .050 inch from the rigid wall.

B. EXPERIMENTAL PROCEDURE

The developing mean velocity profile was monitored at existing ports in the Lucite pipe located at 20, 40, 56, and 272 diameters downstream of the entrance. The quantitative data was recorded at these four stations for Reynolds Number values ($R = U_{MAX} r/\nu$) of 2848 and 5398 respectively.

The fluctuating pressure differentials for high and medium mass flows were obtained using BRUEL & KJAER $\frac{1}{4}$ inch condenser microphones (Model 4136). The mean pressure differentials were obtained using micro manometers.

To measure the pulsating velocity components, the cross wire probe was installed at station 1, twenty diameters downstream of the entrance. Radial distribution of velocity amplitudes and phase shifts were taken at sinusoidal pressure oscillations of 15 cps and 20 cps and at high and medium mass flow rates. All time-dependent data were recorded on a

two-channel Sanborn Model 296 recorder. The physical setup of the electronic equipment utilized to measure the oscillating velocity components and pressures is shown in Figure 2.

On the two-channel recorder $\tilde{v}$ and $\tilde{u}$ data was recorded alternatively; the input pressure signal was continuously monitored.

C. EXPERIMENTAL RESULTS

Initially, mean flow velocity data was evaluated at station 1 where the oscillating velocity determinations were to be obtained. A smooth curve was fitted to the mean flow data by the least squares method. Figures 3 and 4 illustrate the computed plots for flow Reynolds Numbers of 2848 and 5348 respectively. Table III gives the numerical results for the developing velocity profile at the succeeding stations.

Secondly, verification of the phase shift, ϕ, inherent in the radial velocity expression was sought. After choosing an arbitrary $t = 0$ setting upon the records of the pressure and velocity signals, a subsequent marking of parallel times allowed for a direct verification of analytical values as shown by the representative tracings in Figures 13 and 14 for a pulsation frequency of 20 cps. While equipment limitations forbid a conclusive verification at this frequency; nevertheless, the appearance of the 90 degree phase shift between the axial velocity and pressure signals on the centerline which is evidenced in Figure 15 and which is also predicted by theory makes the radial results less tentative.

Finally, a comparison of theoretical and experimental values for both radial and axial fluctuation velocity components was determined as shown in Figures 5-12. In the case of the axial velocity component, the comparison between experimentally measured values and theoretically calculated values is direct whereas for the radial velocity component the theoretical curves incorporated an arbitrary amplitude factor.

IV. CONCLUSION

The final theoretical conclusions follow from the anamolous physical situation represented by equation (28) which demonstrates the viscous decay of the radial velocity component. Removing the x dependence of $\tilde{v}$, removed the production term $(\bar{u} \frac{\partial \tilde{v}}{\partial x})$ which was necessary to generate the $\tilde{v}$ term initially. Thus, subsequent theoretical determinations are made upon a velocity component which is not strictly allowed by the linear analysis pursued. This anamoly is represented by the appearance of the arbitrary constant in the final expression for the radial velocity component.

A second manifestation of this anamoly is evident in the independence of time that exists in the final expression for $\tilde{v}$ since

$$(nt+\phi) = \tan^{-1} \mathrm{ber}_1 x_0 / \mathrm{bei}_1 x_0 \quad .$$

Thus the initial form of $\tilde{v}$ which follows from this result must persist. Both the form and persistence (since RMS evaluations are involved) seem to be suggested by the comparison of the theoretical and experimental values for the radial velocity component portrayed in Figures 9-12. Again it is to be noted that the theoretical curves here incorporate an arbitrary amplitude factor. However, as in all linear eigenvalue

problems, it is the form rather than the absolute value of the eigenfunction which is important and which is verified experimentally here.

The comparison of values in the case of the axial velocity component as expressed in Figures 5-8 is more conclusive. This data, though limited in nature verifies previous (Richardson [9]), theoretical and experimental determinations and thus helps substantiate the parallel radial data which was simultaneously recorded.

These mean determinations portray another characteristic of pulsatory flows, namely, that the maximum mean flow does not occur at the center of the pipe but in a region near the wall. The location of this region approaches the wall as pulsation frequency increases. As evidenced in both the radial and axial data, the high value of the argument in the Bessel functions involved in the velocity expressions makes the wall area values predominant. Thus the central portion of the flow is recognized as being practically unaffected by pulsation. Moreover, the value of axial fluctuation velocity is a non-zero constant on the pipe axis - another result verified by the data in Figure 5-8. In contrast, the zero value of radial velocity fluctuation on the pipe axis is evidenced by Figure 16 which portrays the radial velocity component recorded with the same gain readings as pertain to all other tracings shown. The appearance of this figure is that of a filtered noise signal and demonstrates the favorable signal to noise ratio evidenced by the other recorded data.

In addition to the results concerning the existence of a radial fluctuation velocity component, the second new result warranted by the accompanying analysis was the appearance of a frequency dependent phase shift in the formulation of this velocity component. Results concerning this phase shift are shown in Figures 13 and 14 where determinations for t = 0 values approach those values of phase shift suggested by the analysis for a pulsation frequency for 20 cps. Equipment limitations did not allow verification of non-zero time values. However, as stated previously, the appearance of a 90 degree phase shift in the axial velocity and pressure data recorded in Figure 15 tends to substantiate the companion radial velocity data.

In conclusion, the limited experimental program reported here only demonstrates trends toward the parallel theoretical determinations. A more comprehensive experimental program would require both new electronic filters with band pass capabilities in the .01 cps range and a new pressure monitoring device to replace the microphone system which has severely attenuated response below 20 cps. In view of these requirements, a re-evaluation of analytical results is recommended before a more extensive experimental phase is commenced.

TABLE I

Constants for series solution of $\tilde{v}$; solution # 1 of the Pulsating Flow equations.

1. $$\lambda_1 = \frac{C_1 a_0 b_0 e^{-\omega^2 x_\pi}}{\nu}$$

2. $$\lambda_2 = \frac{C_1 a_0 b_1 e^{-\omega^2 x_\pi}}{\nu(-i)^{1/2}\lambda}$$

3. $$\lambda_3 = \frac{2C_1 a_0 b_0 B_2 e^{-\omega^2 x_\pi}}{\nu\, i\, \lambda^2}$$

4. $$\lambda_4 = \frac{C_1 a_0 \pi e^{-\omega^2 x}}{2\,\nu\,(-i)^{3/2}\,\lambda^3}\ (-3b_1B_2 - 5b_0B_3)$$

5. $$\lambda_5 = \frac{C_1 a_0 \pi e^{-\omega^2 x}}{\nu\,\lambda^4}\ (3b_0B_4 + 2b_1B_3 + 2b_2B_2)$$

6. $$\lambda_6 = \frac{C_1 a_0 \pi e^{-\omega^2 x}}{2 \times \lambda^5 (-i)^{1/2}}\ (7b_0B_5 + 5b_1B_4 + 3b_2B_3)$$

7. $$\lambda_7 = \frac{C_1 a_o \pi e^{-\omega^2 x}}{\nu\,\lambda^6\, i}\ (-4b_0B_6 - 3b_1B_5 - 2b_2B_4)$$

8. $$\lambda_8 = \frac{C_1 a_0 \pi e^{-\omega^2 x}}{2 \nu \lambda^7 (-i)^{3/2}} (9b_0 B_7 + 7b_1 B_6 + 5b_2 B_5)$$

9. $$\lambda_9 = \frac{C_1 a_0 \pi e^{-\omega^2 x}}{\nu \lambda^8} (-5b_0 B_8 - 4b_1 B_7 - 3b_2 B_6)$$

TABLE II

Constants for $\tilde{v}$ independent of x solution; solution # 2 of the Pulsating Flow equations.

1. $$\lambda_{21} = \frac{C_4 U_0 \pi \sqrt{-i}}{r_0^2 \sqrt{n\nu}}$$

2. $$\lambda_{22} = \frac{C_4 U_0 \pi \sqrt{-i}}{4\nu} \left(\frac{N}{\nu}\right)^{1/2}$$

3. $$\lambda_{23} = \frac{C_4 U_0 \pi \sqrt{-i}}{4 r_0^2 \sqrt{n\nu}}$$

4. $$\lambda_{24} = \frac{C_4 U_0 \pi \sqrt{-i}}{2\ \nu} \left(\frac{N}{\nu}\right)^{1/2}$$

5. $$\lambda_{25} = \frac{C_4 U_0 \pi \sqrt{-i}}{2 r_0^2 \sqrt{n\nu}}$$

TABLE III

Coefficients of the polynomial approximations to the velocity profiles of the form:

$$\frac{\bar{u}}{U_M} = b_0 + b_1\left(\frac{r}{r_0}\right) + b_2\left(\frac{r}{r_0}\right)^2 + b_3\left(\frac{r}{r_0}\right)^3$$

x/d	mass flow rate	b_0	b_1	b_2	b_3
20	high	0.9915	-.0964	1.3958	-2.4025
	medium	0.9760	.3159	-.1252	-1.2745
40	high	1.0137	-.4726	2.3368	-2.9733
	medium	0.9804	-.1590	0.5294	-1.7836
56	high	1.0010	-.1717	1.3127	-2.1629
	medium	0.9996	-.1579	0.9104	-1.8154
272	high	0.9653	.6795	1.6906	-0.0106
	medium	0.9904	.1320	-1.5630	0.4163

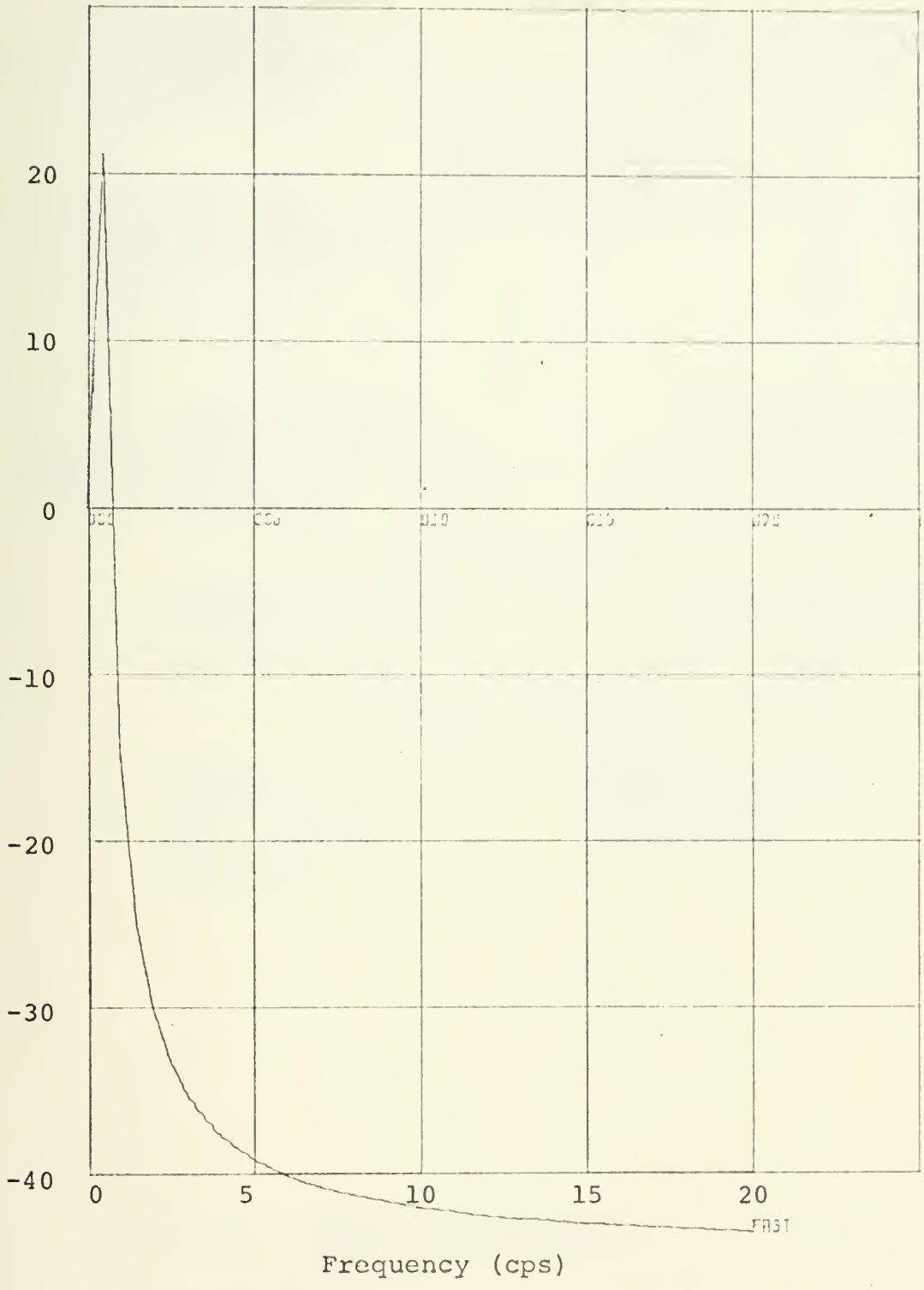

Figure 1. Phase Shift (degrees) vs Frequency (cps) of $\tilde{v}$ compared with pressure signal at t = 0.

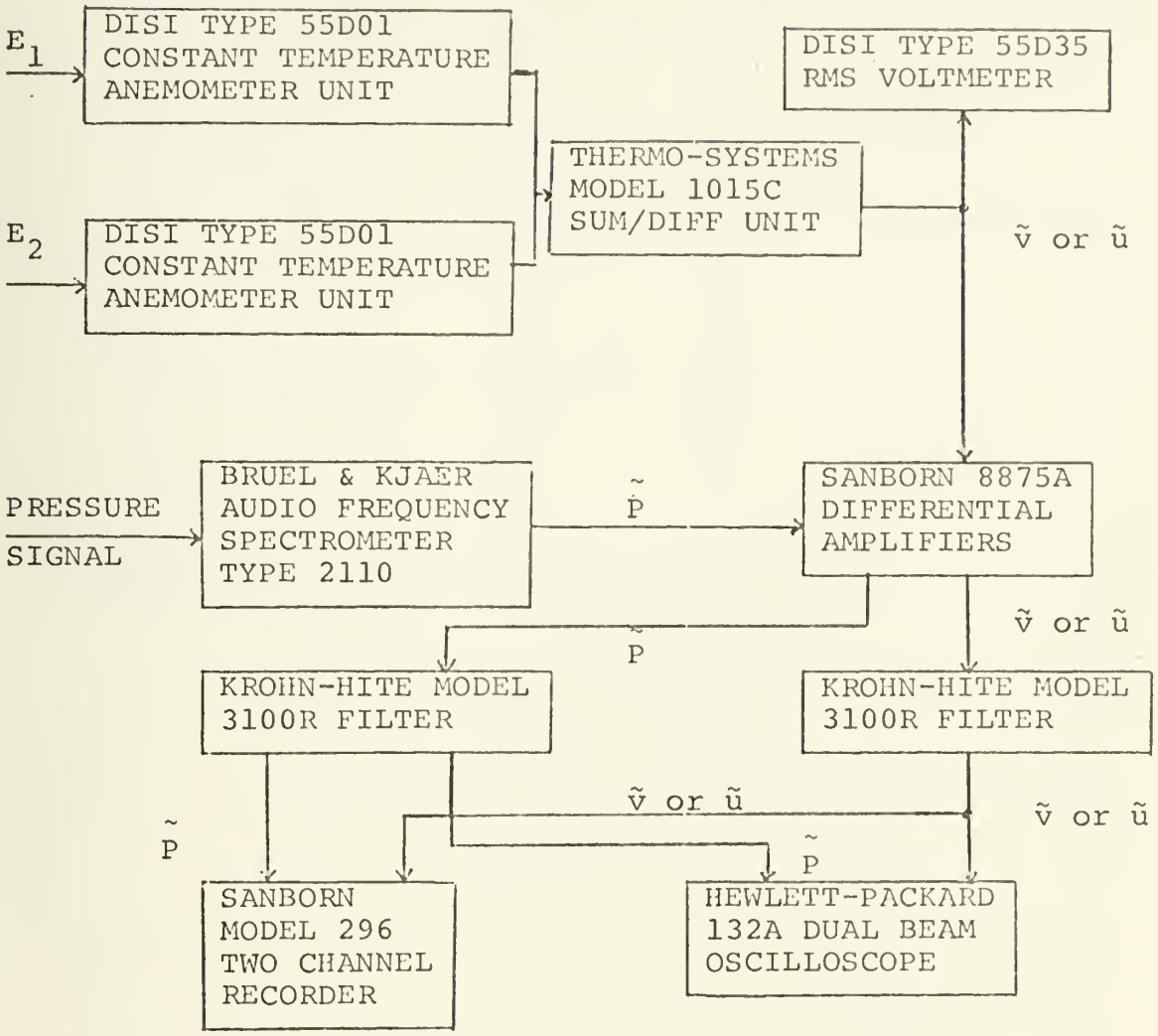

Figure 2. Physical arrangement of electronic equipment for measuring $\tilde{u}$, $\tilde{v}$, and $\tilde{p}$.

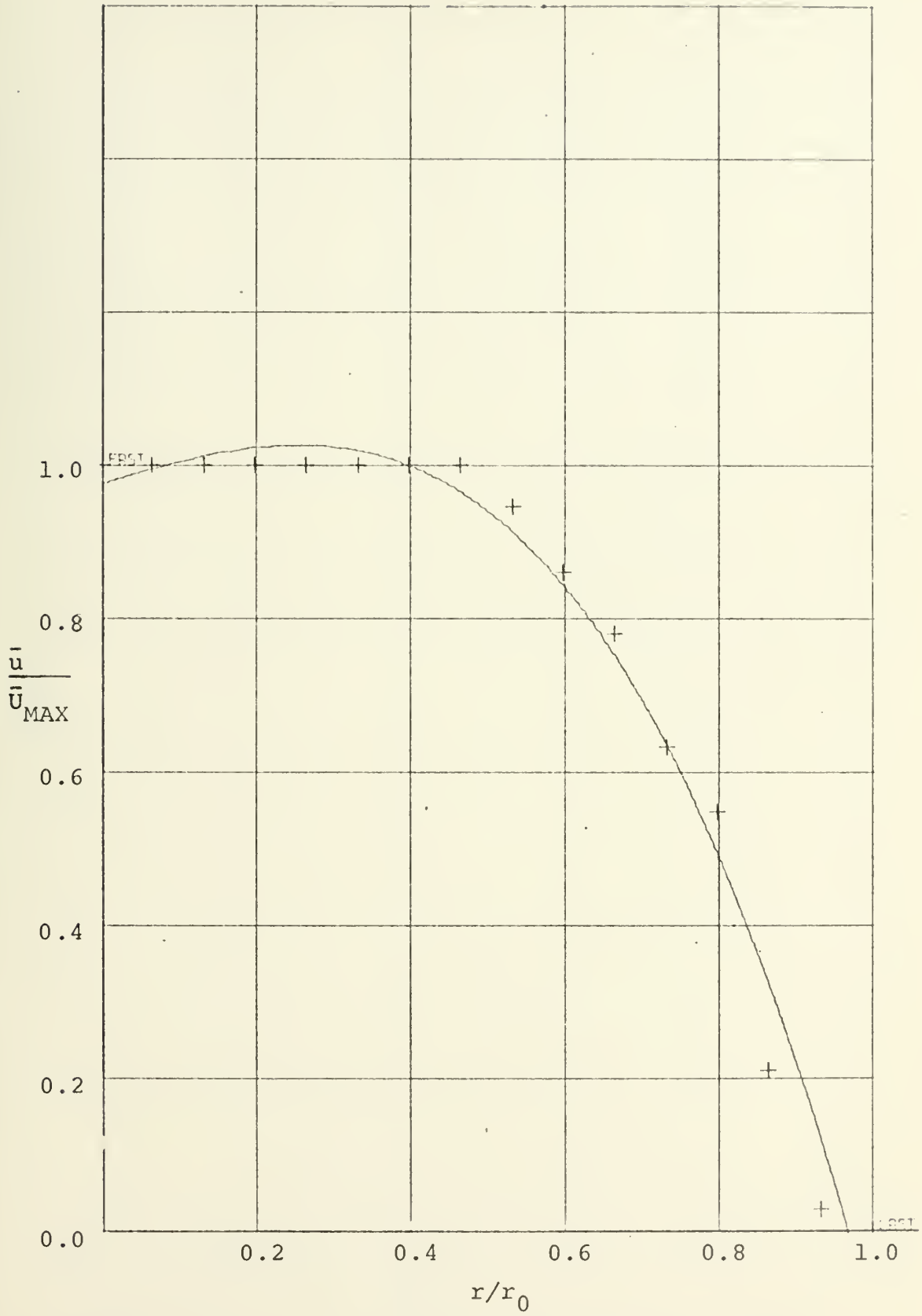

Figure 3. Developing Velocity Profile; x/d=20, R=2848.

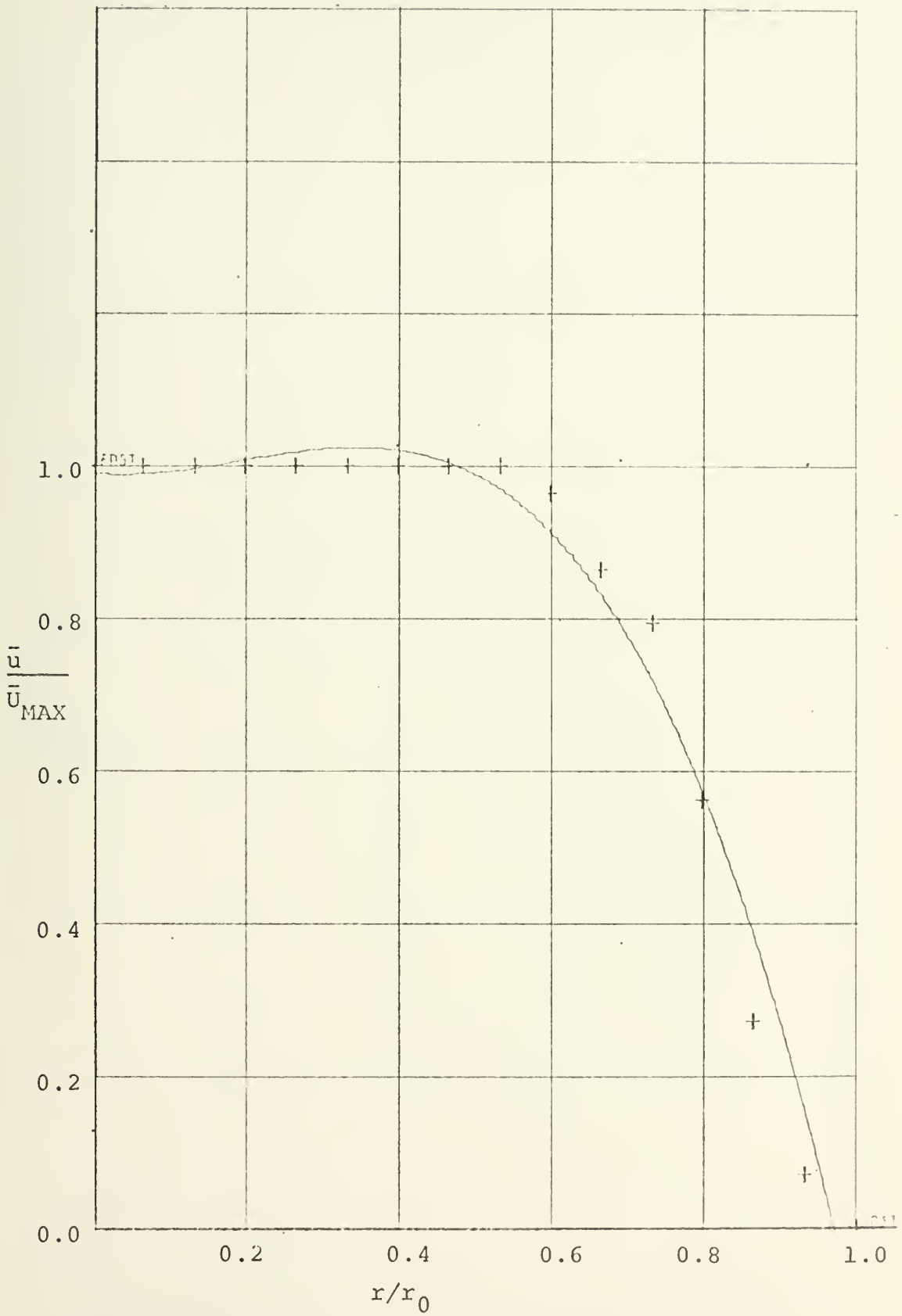

Figure 4. Developing Velocity Profile; x/d=20, R=5348.

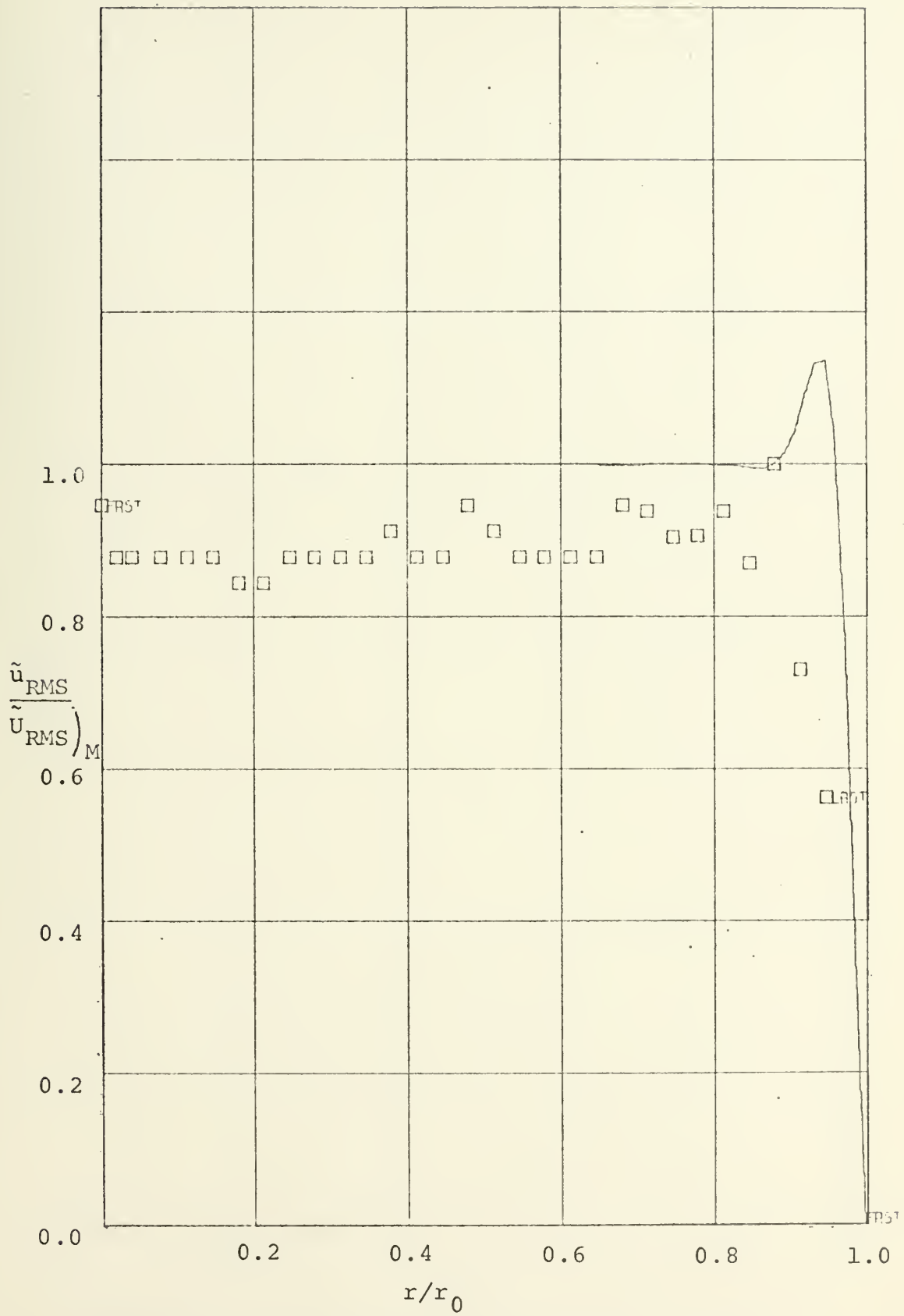

Figure 5. Axial Velocity Component; R=5348, Freq = 20 cps.

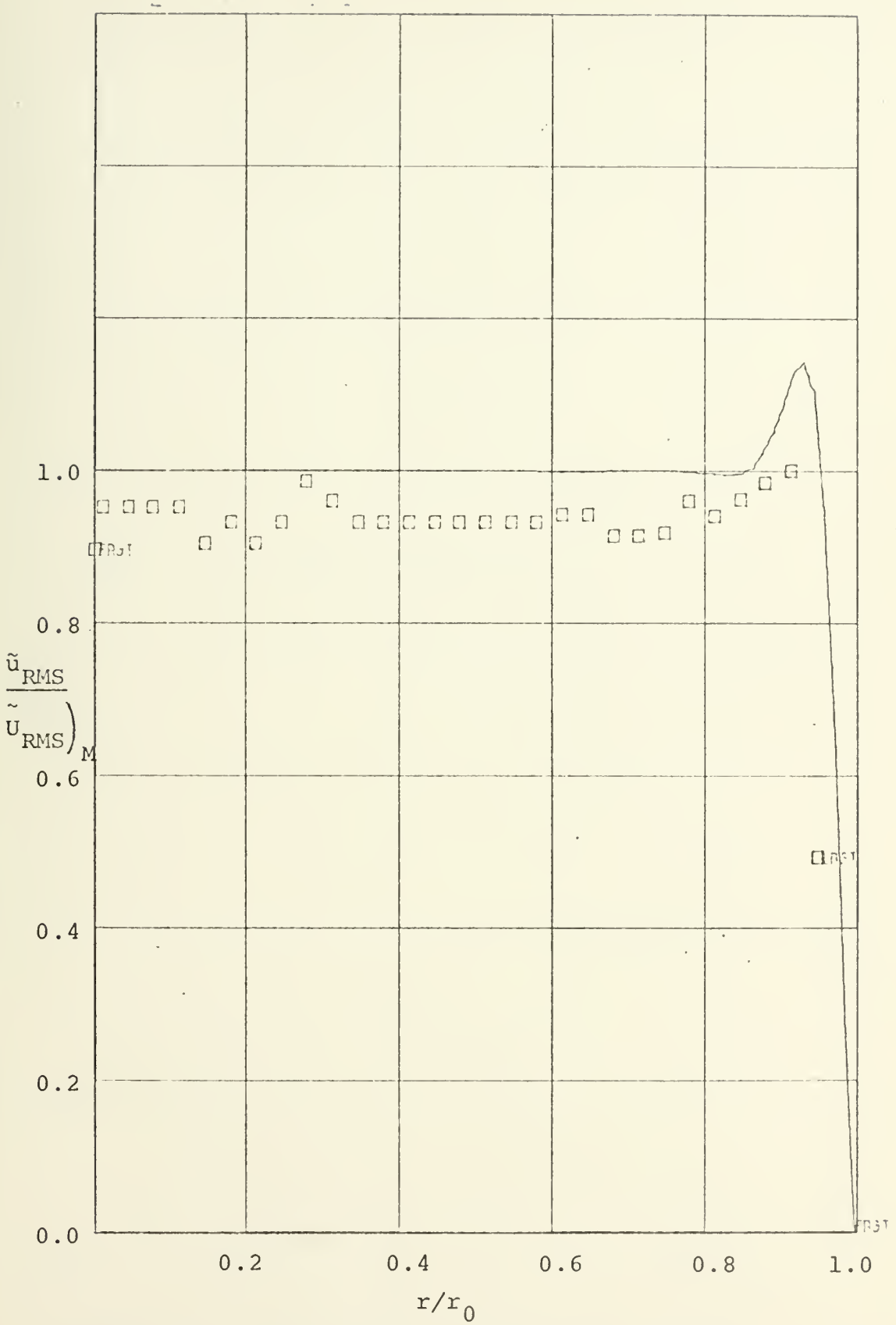

Figure 6. Axial Velocity Component; R=5348, Freq = 15 cps

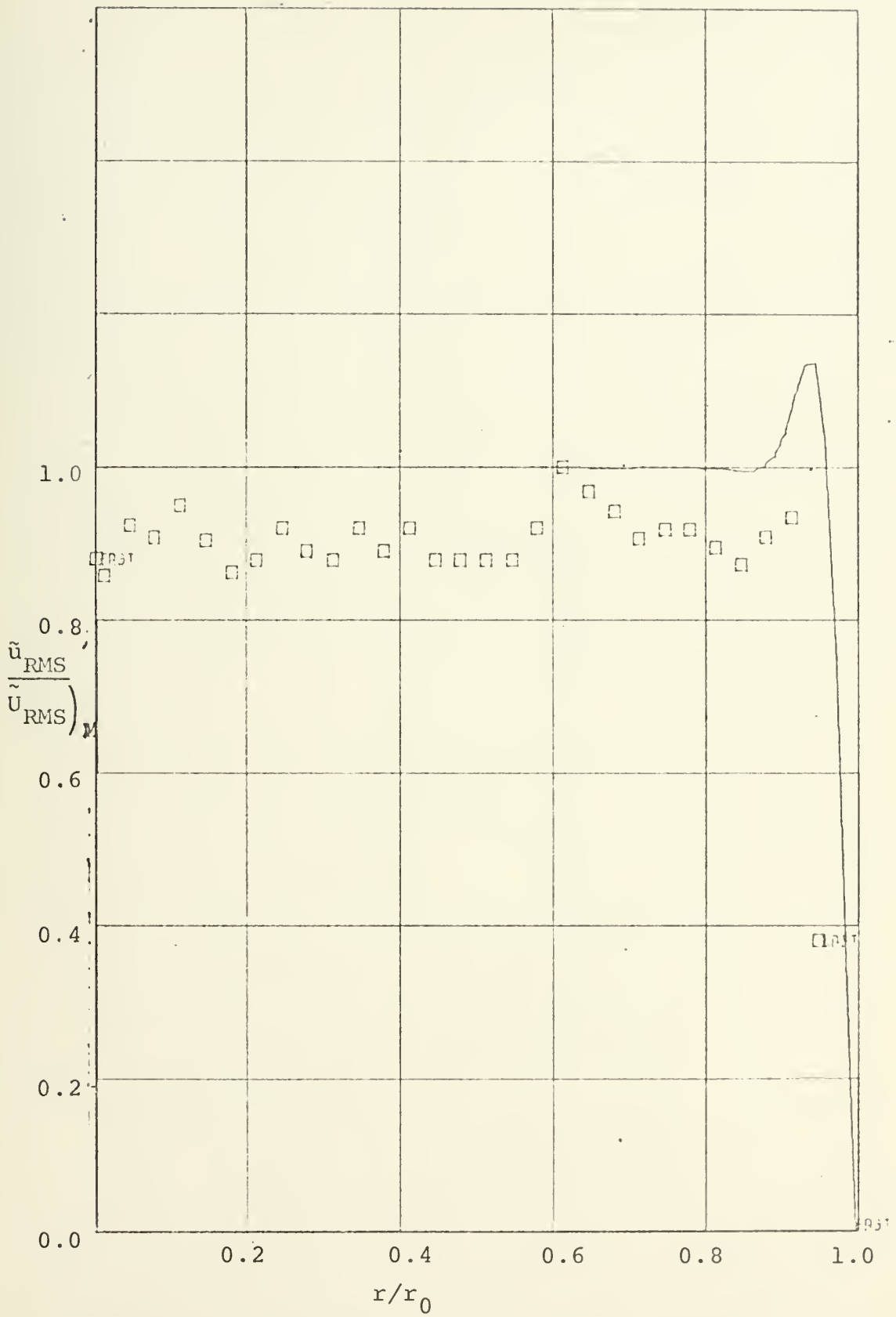

Figure 7. Axial Velocity Component; R=2848, Freq = 15 cps.

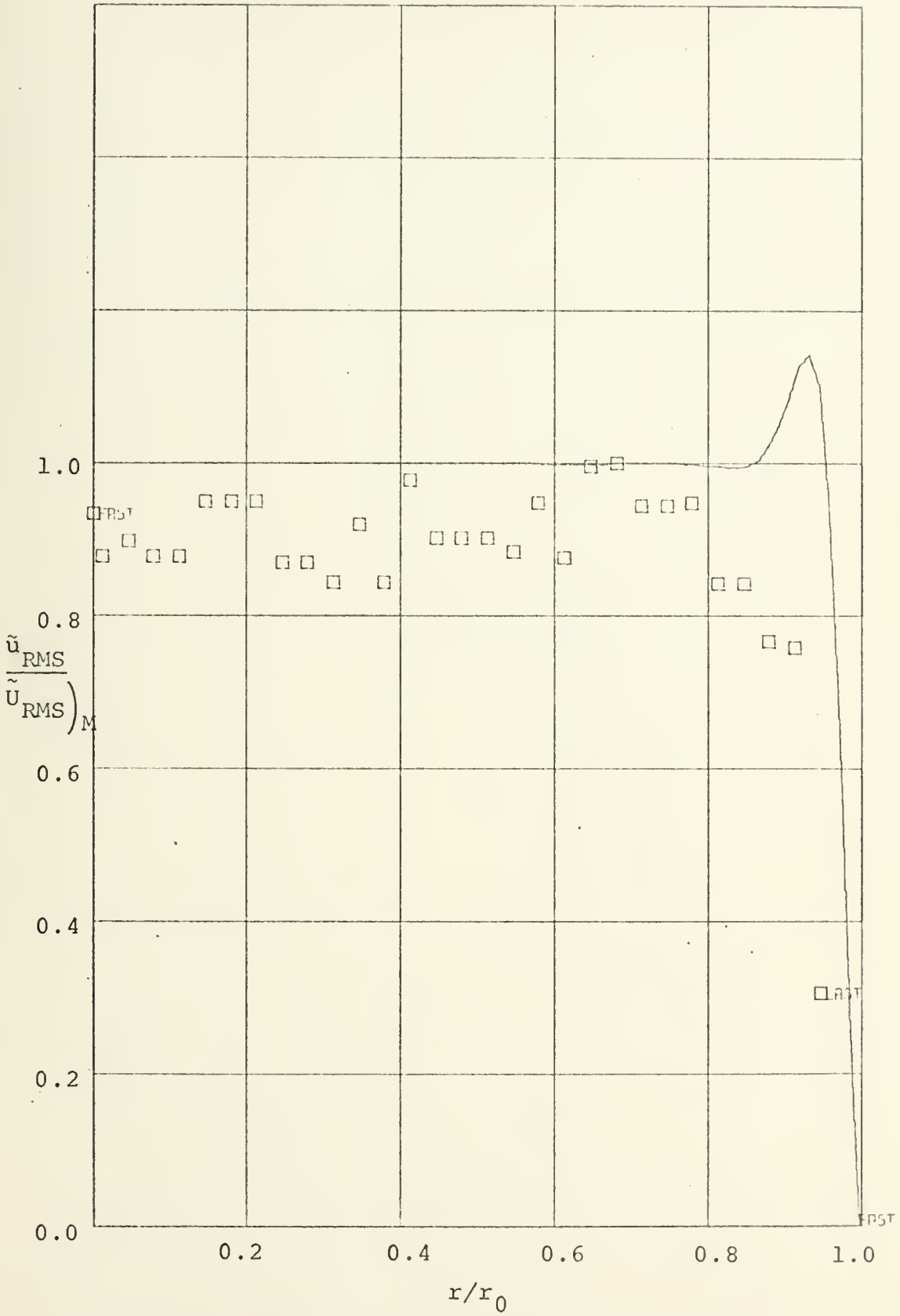

Figure 8. Axial Velocity Component; R=2848, Freq = 15 cps.

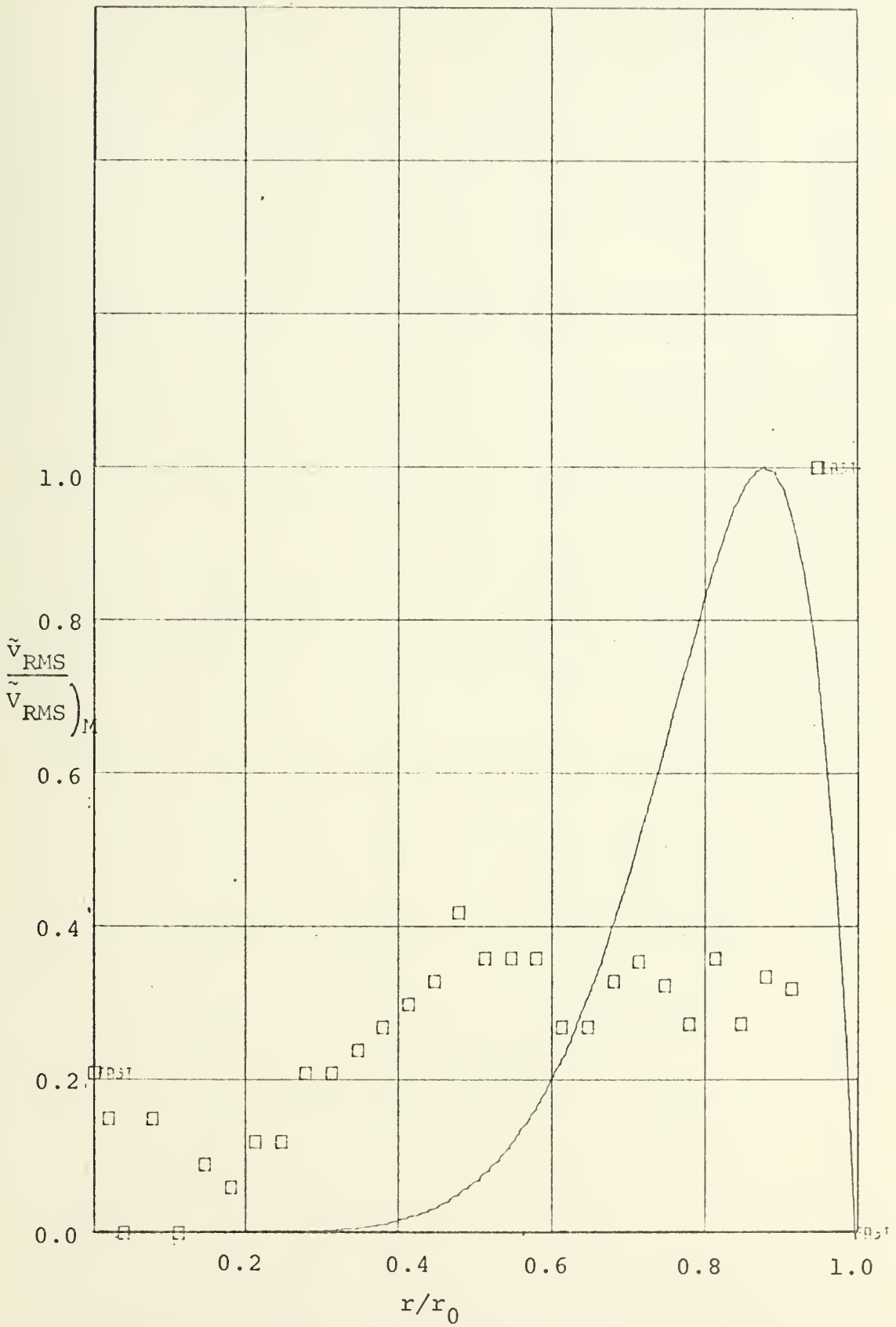

Figure 9. Radial Velocity Component; R=5348, Freq = 20 cps.

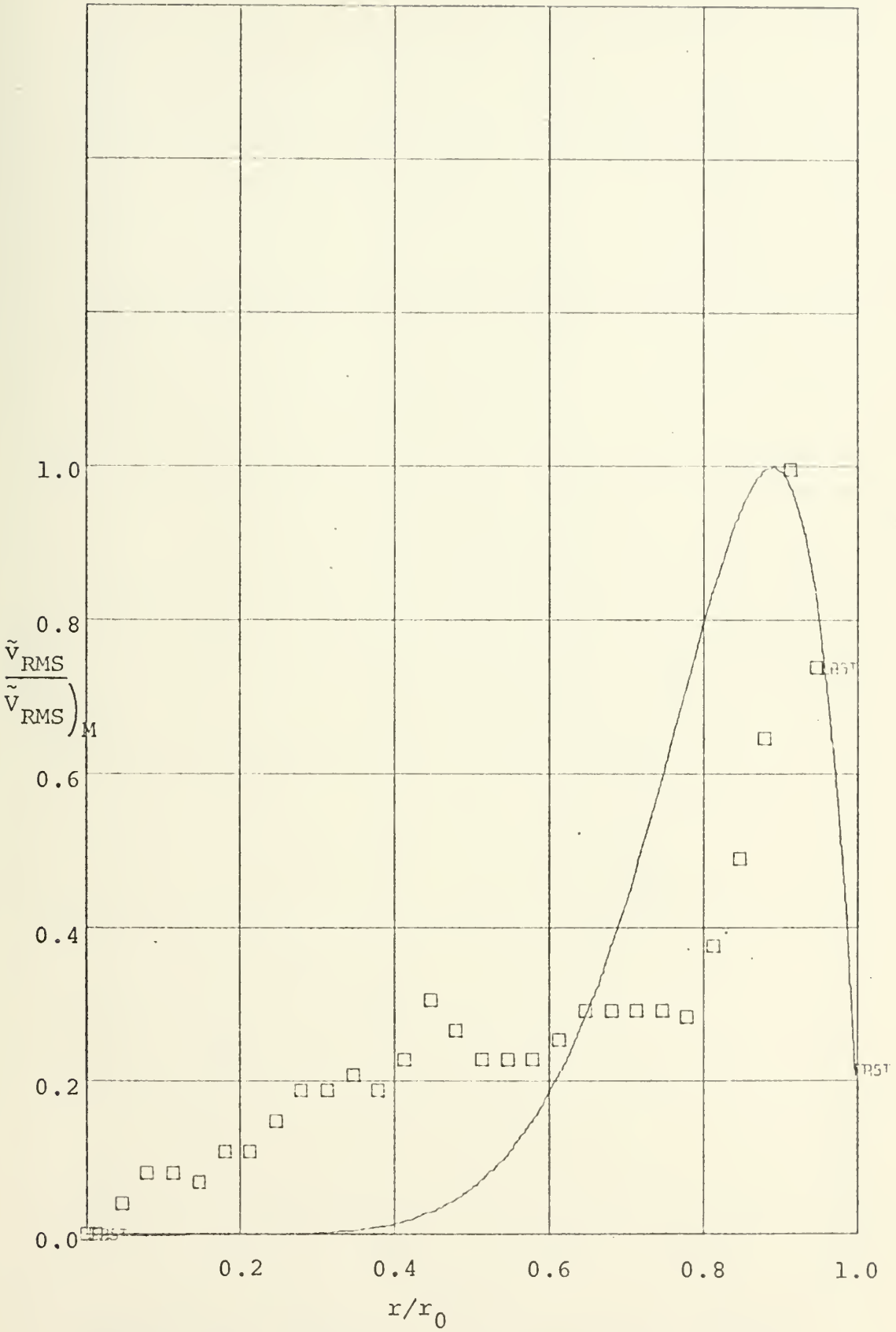

Figure 10. Radial Velocity Component; R=5348, Freq = 15 cps.

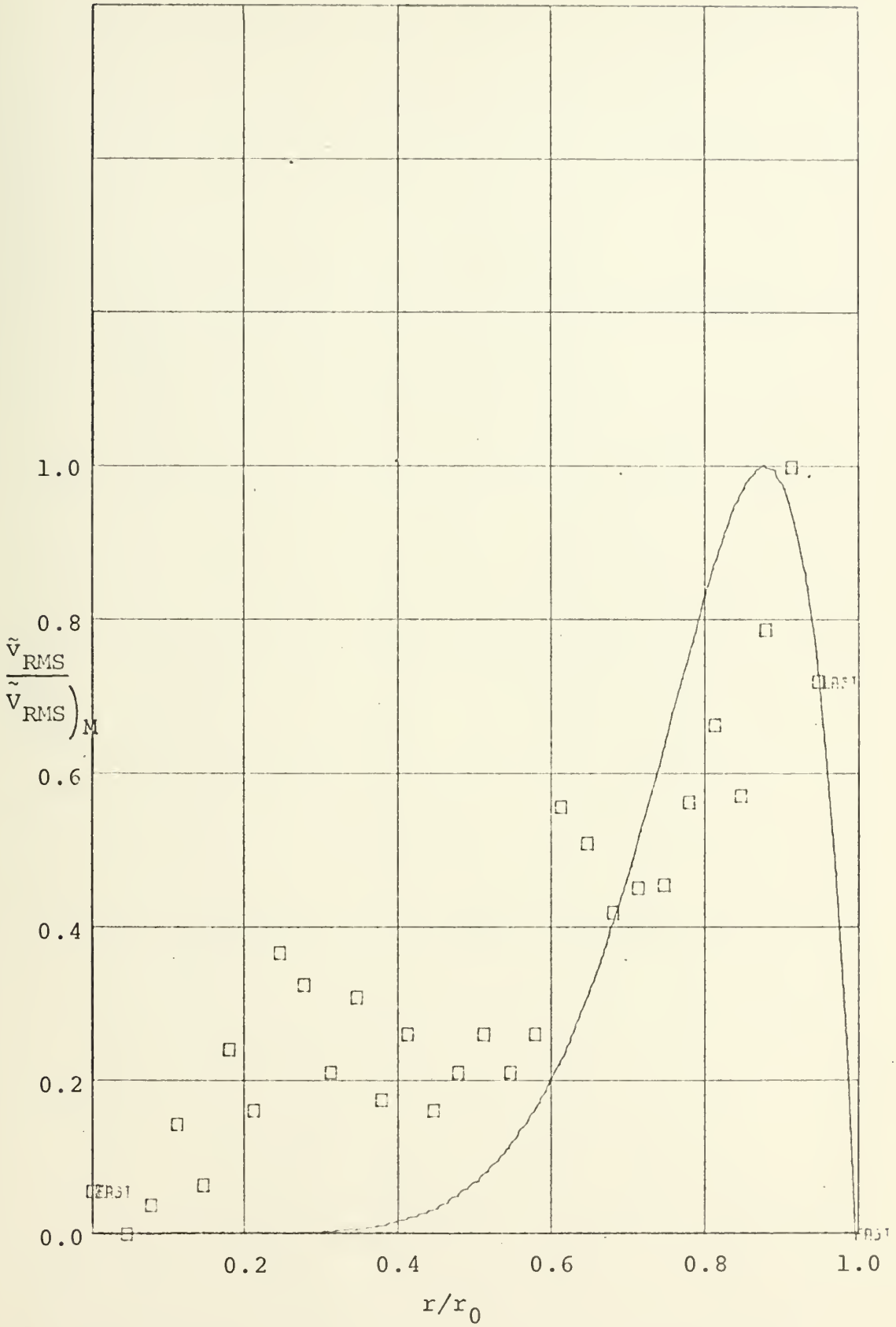

Figure 11. Radial Velocity Component; R=2848, Freq = 20 cps.

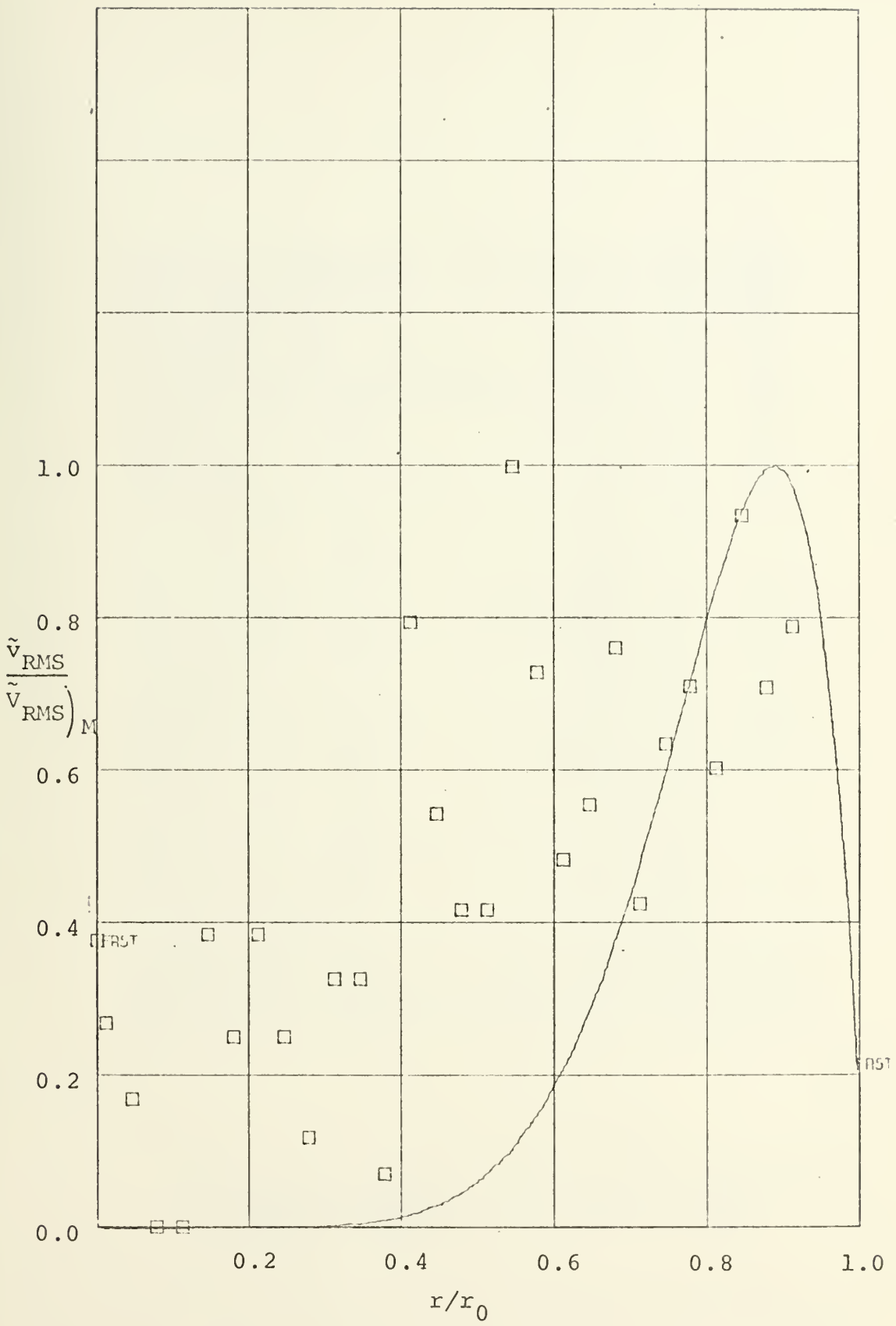

Figure 12. Radial Velocity Component; R=2848, Freq = 15 cps.

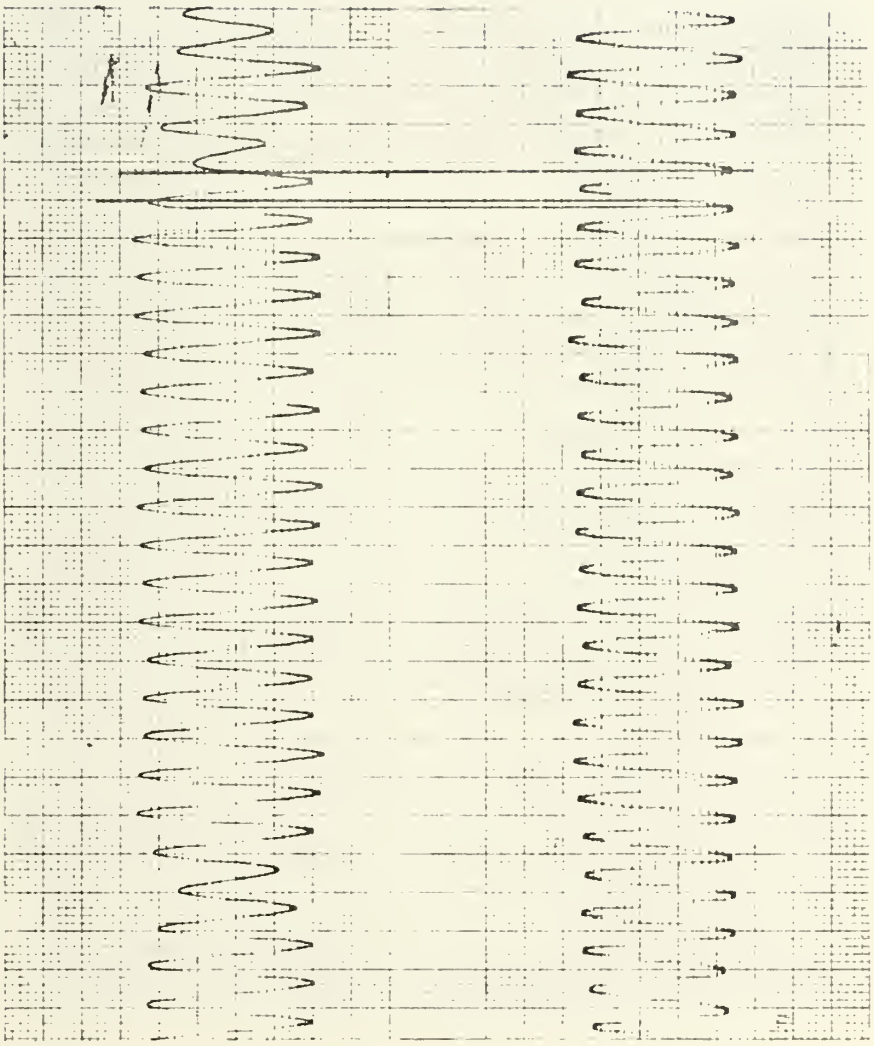

Figure 13. Recorder Tracing of $\tilde{p}$ (left) and $\tilde{v}$ (right) Radius = 0.7, R=2848, Freq = 20 cps, $\phi \approx 45°$.

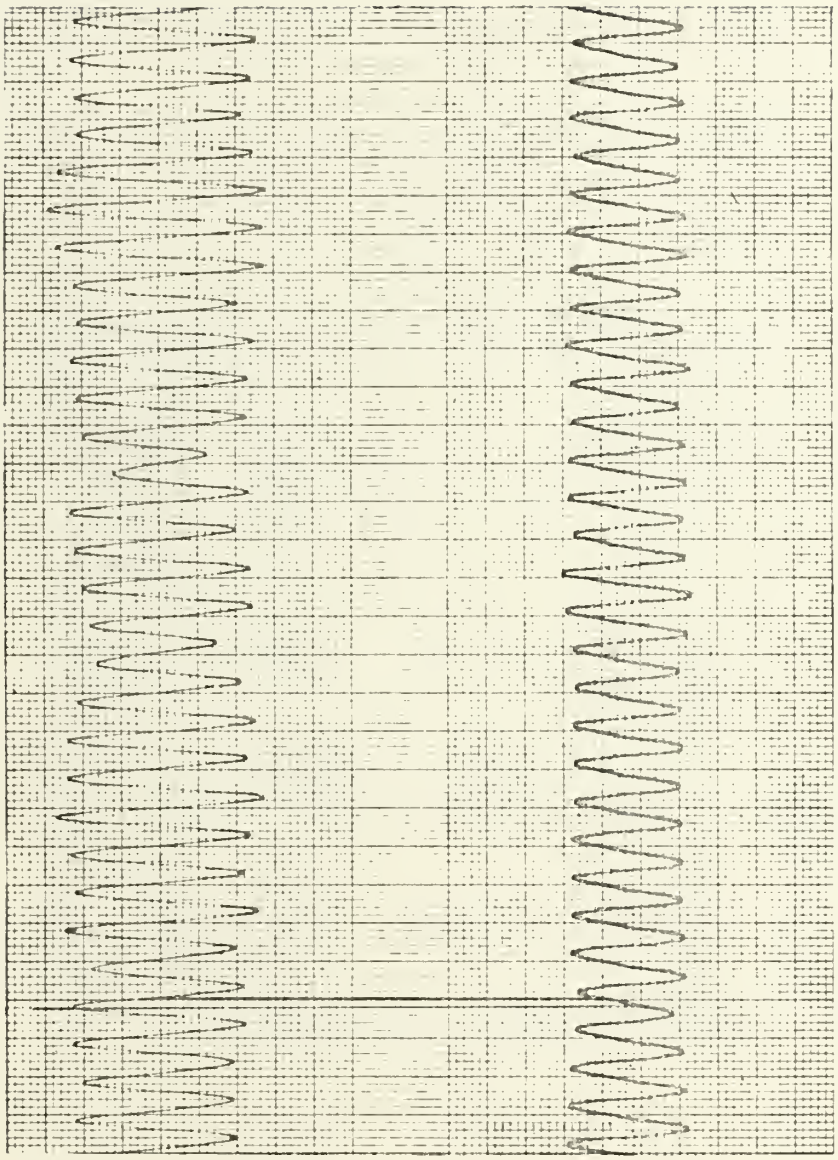

Figure 14. Recorder Tracing of $\tilde{p}$ (left) and $\tilde{v}$ (right) Radius = 0.7, R=5348, Freq = 20 cps, $\phi \approx 45°$.

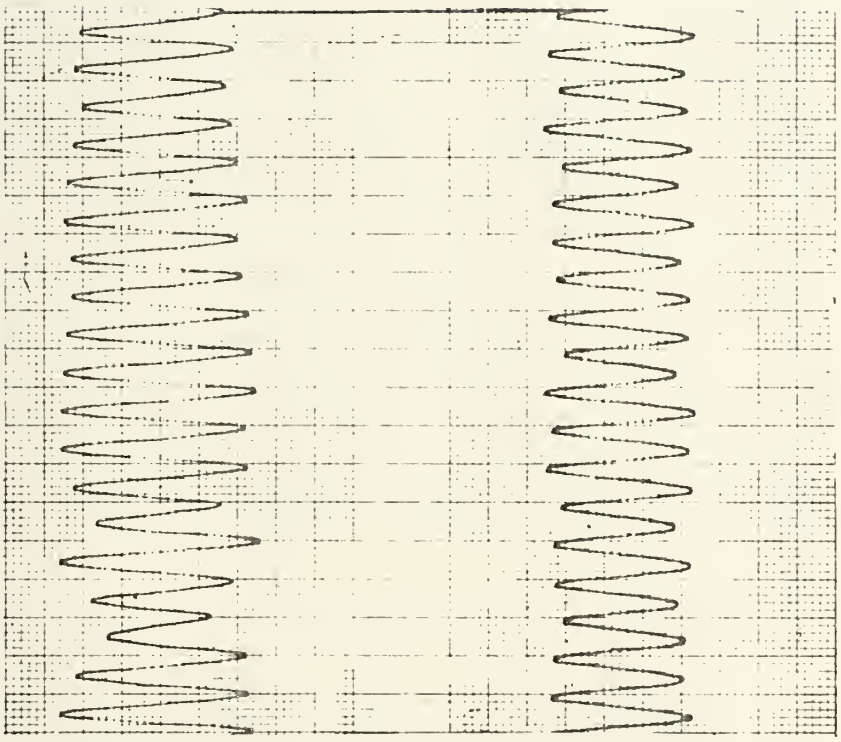

Figure 15. Recorder Tracing of $\tilde{p}$ (left) and $\tilde{u}$ (right) Radius = 0.0, R=5348, Freq = 20 cps, $\phi \approx 90°$.

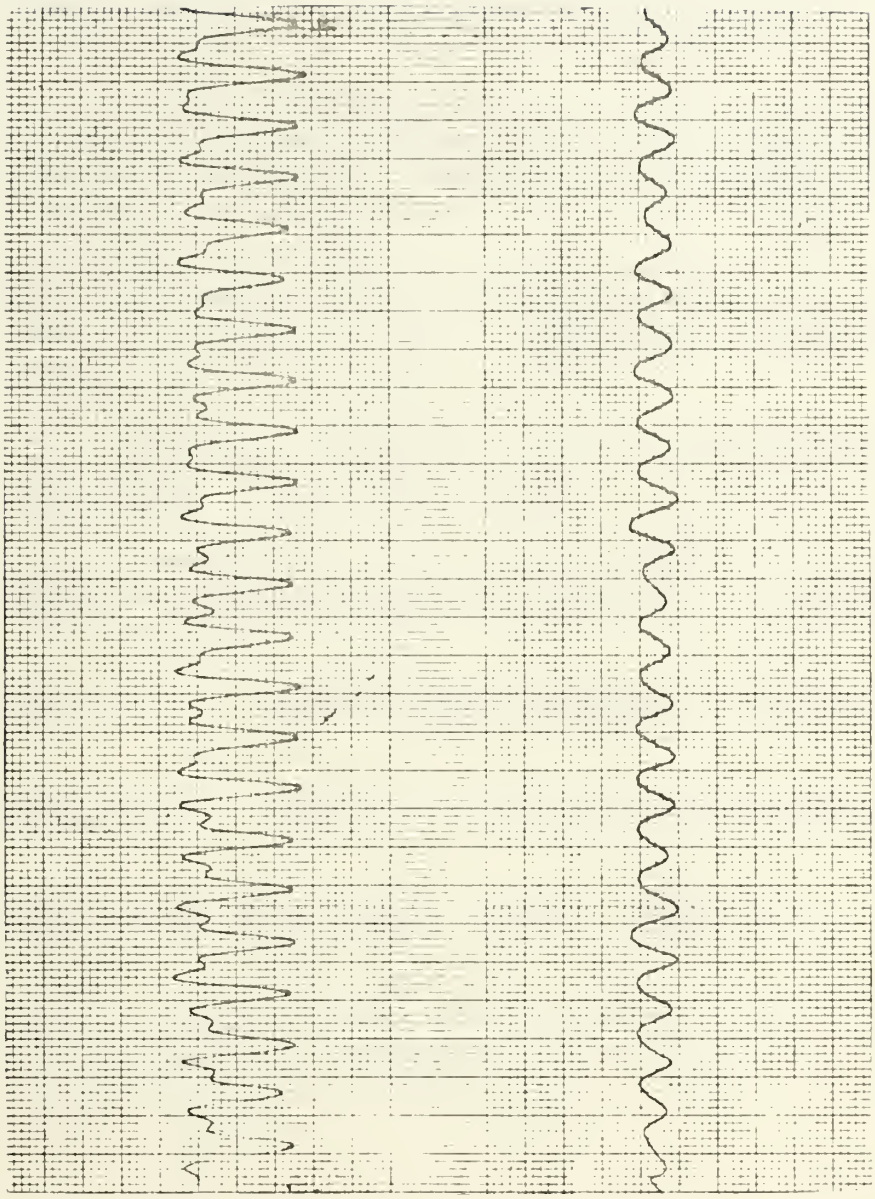

Figure 16. Recorder Tracing $\tilde{p}$ (left) and $\tilde{v}$ (right) Radius = 0.0, R=5348, Freq = 15 cps, $\tilde{v} \approx 0$.

BIBLIOGRAPHY

1. Sexl, Th., "Uber den von E. G. Richardson entdeckten 'Annulareffekt'," Zeitschrift für Physik, v. 61, p. 349, 1930.

2. Uchida, S., "The Pulsating Viscous Flow Superposed on the Steady Laminar Motion of Incompressible Fluid in a Circular Pipe," Zeitschrift für angewandte Mathematik und Physik, v. 7, p. 377, 1956.

3. Atabek, H. B., Chang, C. C., and Fingerson, L. M., "Measurement of Laminar Oscillating Flow in the Inlet of a Circular Tube," Physics of Medicine Biology, v. 9, p. 219, 1964.

4. Florio, P. J., Jr., and Mueller, W. K., "Development of a Periodic Flow in a Rigid Tube," Journal of Basic Engineering, September, 1968.

5. Lew, H. S., and Fung, Y. C., "Entry Flow Into Blood Vessels at Arbitary Reynolds Number," J. Biomechanics, v. 3, p. 23-38, 1970.

6. Schlichting, H., Boundary Layer Theory, McGraw-Hill, 1960.

7. Wylie, C. R., Jr., Advanced Engineering Mathematics, McGraw-Hill, 1960.

8. Abramowitz, M., and Stegun, I. A., Handbook of Mathematical Functions, Dover, 1965.

9. Richardson, E. G., and Tyler, E., "The Transverse Velocity Gradient Near the Mouths of Pipes in Which an Alternating or Continuous Flow of Air Is Established," Proc. Phys. Soc., London, v. 42, p. 1-15, 1929.

INITIAL DISTRIBUTION LIST

		No. Copies
1.	Defense Documentation Center Cameron Station Alexandria, Virginia 22314	2
2.	Library, Code 0212 Naval Postgraduate School Monterey, California 93940	2
3.	Professor T. M. Houlihan Mechanical Engineering Department Naval Postgraduate School Monterey, California 93940	1
4.	LCDR B. P. Whitehurst, USN 605 East Bradford Street Marion, Indiana 46952	1

Security Classification

DOCUMENT CONTROL DATA - R & D

(Security classification of title, body of abstract and indexing annotation must be entered when the overall report is classified)

ORIGINATING ACTIVITY (Corporate author)

Naval Postgraduate School
Monterey, California 93940

2a. REPORT SECURITY CLASSIFICATION

Unclassified

2b. GROUP

REPORT TITLE

Velocity Determinations in Pulsating Pipe Flows

DESCRIPTIVE NOTES (Type of report and inclusive dates)

December 1970

AUTHOR(S) (First name, middle initial, last name)

Byron Paul Whitehurst

REPORT DATE	7a. TOTAL NO. OF PAGES	7b. NO. OF REFS
December 1970	51	9

CONTRACT OR GRANT NO.	9a. ORIGINATOR'S REPORT NUMBER(S)
PROJECT NO.	
	9b. OTHER REPORT NO(S) (Any other numbers that may be assigned this report)

DISTRIBUTION STATEMENT

This document has been approved for public release and sale; its distribution is unlimited.

SUPPLEMENTARY NOTES	12. SPONSORING MILITARY ACTIVITY
	Naval Postgraduate School Monterey, California 93940

ABSTRACT

A study of the fluctuating velocity field in the developing region of a pulsating pipe flow is presented.

Theoretically, three separate determinations of radial and axial perturbation velocity profiles were calculated involving varying degrees of analytical simplication.

Experimentally, pulsating disturbances were created by a sinusoidal pressure wave exciter installed at the outlet of a 1.5 inch circular wind tunnel facility. Cross-wire anemometer measurements of the pulsating velocity components compared favorably with the parallel theoretical results. Likewise, experimental determinations of the phase angles between velocity and pressure signals compared favorably with analytical values.

DD FORM 1 NOV 68 1473 (PAGE 1)

S/N 0101-807-6811

Security Classification

A-31

14 KEY WORDS	LINK A		LINK B		LINK C	
	ROLE	WT	ROLE	WT	ROLE	WT
Pulsating Pipe Flows						

Thesis
W5556
c.1
Whitehurst
Velocity determinations in pulsating pipe flows.
124764